Biochimica et Biophysica Acta 940 (1988) 255–265
Elsevier

BBA 73994

Linear dichroism and orientational studies of carotenoid Langmuir-Blodgett films

Christophe N. N'soukpoé-Kossi [a], Jan Sielewiesiuk [b], Roger M. Leblanc [a], Richard A. Bone [c] and John T. Landrum [c]

[a] *Centre de recherche en photobiophysique, Université du Québec à Trois-Rivières, Trois-Rivières, Québec (Canada),* [b] *Uniwersytet Marii Curie-Sklodowskiej, Instytut Fizyki, Lublin (Poland) and* [c] *Florida International University, Departments of Physics and Chemistry, Miami, FL (U.S.A.)*

(Received 6 November 1987)

Key words: Carotenoid; Linear dichroism; Langmuir-Blodgett film; Macula; Haidinger brush; Henlé fiber; (Retina)

The linear dichroism of single monolayers of lutein, zeaxanthin and a mixture of lutein and synthetic phosphatidylcholine has been measured. The angle of orientation of the carotenoid molecules was found to lie between 45° and 51° relative to the plane of the solid support. Although the adsorbed monolayers were mostly in a monomeric state, microscopic observations, as well as the Π-A isotherms, indicated the existence of crystalline islets. The results have been interpreted in connection with Haidinger's polarization brushes.

Introduction

Carotenoids are supposed to act as photoprotective pigments in photosynthetic membranes, and possibly also in the primate retina [1–7]. In addition, they have been assigned another role in the retina, as an optical filter for reducing the effects of chromatic aberration [8–10], the main concern of this paper.

The carotenoids in human retina have been identified as lutein and zeaxanthin [11] responsible for the yellow colour of the retinal macula, the site of localization of the structure responsible for Haidinger's brushes [12–14]. The brushes are attributed to the directional organization of carotenoids in the membranes of Henlé's fibers (the inner segments of cone receptor cells [15]).

A number of studies have been published concerning the orientation of carotenoids in vivo [16–20] and in vitro [21–27], but many conflicting hypotheses have emerged. Some authors concluded that carotenoids are oriented parallel to the bilayer plane in vesicles [21,22] and in chloroplasts [16–19] or traverse it perpendicularly in liposomes [23]. From resonance Raman studies on lipid bilayers, Van de Ven et al. [27] found that β-carotene is oriented parallel to the lamellar plane in dioleoylphosphatidylcholine bilayers but perpendicular to it in soybean phosphatidylcholine bilayers. Results obtained for mixed monolayers of β-carotene and barium stearate led Ohnishi et al. [24] to the conclusion that β-carotene is aligned in the multilayer parallel to the plane of the glass support. Reich et al. [25] and Sewe and Reich [26] noted that carotenoids would lie rather flat in chloroplast membrane, as suggested by results obtained from electrochromic measurements.

In an attempt to resolve these controversies, we have investigated the orientation of carotenoids in a single monolayer state. In the present paper, we

Correspondence: R.M. Leblanc, Centre de recherche en photobiophysique, Université du Québec à Trois-Rivières, C.P. 500, Trois-Rivières, Québec, Canada, G9A 5H7.

report data related to the linear dichroism of monolayers measured at different angles of incidence, the interfacial properties, and the orientation of molecules in pure lutein and zeaxanthin monolayers and of lutein when mixed with a phospholipid. The results obtained indicate clearly that the carotenoids studied lie at a mean angle of 48° to the plane of the solid support, fulfilling the condition for the Haidinger's brushes formation in the macula.

Materials and Methods

Materials

Benzene (BDH Chemicals, Montréal, Québec, Canada) distilled at 80°C in a glass bead column and ethanol (Les Alcools de Commerce Ltée, Ville St-Laurent, Québec, Canada) distilled at 78.5°C in a Vigreux column were used as solvents to prepare carotenoid solutions. For the monolayer work, water was filtered and deionized in a nanopure Barnstead column (Fisher Chem. Co., Montréal, Québec, Canada) to obtain a specific resistivity of 16–18 MΩ cm and was bidistilled in a quartz distiller (Heraeus Quarzschmelze GmbH, Produktbereich Infrarot, Hanau 1, F.R.G.): the surface tension was equal to or higher than 71 $mN \cdot m^{-1}$, pH 5.6. Zeaxanthin was supplied by Hoffman-La Roche Co. (Basle, Switzerland). Lutein was isolated from spinach leaves, its identification and purity being confirmed by high-performance liquid chromatography, thin-layer chromatography, spectral absorbance measurements and mass spectrometry [28–31]. The spectrophotometer used was a Perkin-Elmer 553 (Perkin-Elmer Corporation, Oak Brook, Instrument Division, Oak Brook, IL) provided with a Data Station for computation work. The polarizers used were supplied by A.B.P. Inc. (Montréal, Québec).

Methods

(1) Purification of lutein

Isolation of lutein from spinach was accomplished by the following procedures. Warm methanol extracts were treated with KOH to saponify the chlorophylls, and the carotenoids separated by solvent partition using diethyl ether [29]. Purification and initial identification of the individual carotenoids were done by thin-layer chromatography following the methods of Hager and Meyer-Bertenrath [32]. For large scale work, these methods were adapted to liquid column chromatography. Identification of lutein was confirmed by mass spectrometry, high-performance liquid chromatography, UV-visible spectrometry and chemical derivatization. In all cases, agreement with literature data was obtained [28–31].

(2) Π-A isotherms

Distilled and deionized water was used as the subphase. Spreading solutions of pure lutein, or synthetic phosphatidylcholine, or a mixture of both were prepared as follows: we first dissolved lutein and phosphatidylcholine separately in a benzene/ethanol mixture (9:1, v/v). Both solvents were freshly distilled and bubbled with argon. The two solutions were then mixed to give the required molar ratio of lutein to phosphatidylcholine. As a rule, the concentration of the solutions was $(2–4) \cdot 10^{-4}$ $mol \cdot dm^{-3}$. Solutions were prepared and stored in vials filled with argon and closed with mininert valves (Chromatographic Specialties Ltd., Brockville, Ontario, Canada). All operations with monolayers were performed under a nitrogen atmosphere. In all experiments, the initial molecular area was approximately 200 $Å^2$/molecule. In one series of experiments, the rate of compression was 8 $Å^2$/mol per min, and, in another one, 3 $Å^2$/mol per min, in order to investigate the effect (if any) of the speed of compression on the *Π-A* isotherms.

The measurements were performed on a trough with useful dimensions $50.0 \times 14.0 \times 1.0$ cm equipped with a Langmuir-film balance provided with a DCDT transducer (Hewlett Packard). The movement of the compressing barrier was controlled by an Apple II computer.

(3) Monolayer deposition

The solutions were prepared as previously described. The solid support for the deposition consisted of two quartz disks, 2.54 cm in diameter (Esco Products Inc., Oak Ridge, NJ, U.S.A.) set face-to-face and joined along their rims by paraffin wax. This arrangement allows for the adsorption of one monolayer on only one face of each disk. The support was immersed in the water

subphase contained in the trough (30.0 × 14.7 × 4.5 cm), and the carotenoid solution was spread on the water surface. Operations were carried out under a nitrogen atmosphere. After a 10-min period to allow for homogeneous spreading, the molecules were compressed until the desired surface pressure (e.g. 5, 25 or 40 $mN \cdot m^{-1}$, deposition pressure) was reached. The pure carotenoid monolayers were very unstable at the air/water interface as usually evidenced by a drop in the surface pressure when the compression was stopped and by a deposition ratio higher than 1.2. As soon as the deposition pressure was reached, hydrophilic adsorption of the monolayer was obtained by lifting the support at a speed of 0.6 $cm \cdot min^{-1}$ by means of a vibration-free hydraulic system [33]. During the lifting process, the pressure was maintained at a constant value by adjusting the compression. The quartz disks were then separated, each of them carrying a single monolayer on only one face. The slides were mounted in a special holder which was placed in an aluminum foil-wrapped beaker in the presence of argon. The monolayers were analyzed immediately in the spectrophotometer.

(4) Linear dichroism measurements

All of the absorption spectra were measured under a nitrogen atmosphere at 23–25 °C. The slides were disposed (one at a time) in the spectrophotometer in exactly the same orientation as during the deposition of the monolayer. The absorption spectra were run both in unpolarized and polarized light at angles of incidence, α, of 0°, 45° and 65°. The absorption spectrum of each monolayer in unpolarized light was always checked at the end of each series of measurements.

The linear dichroism, D, was calculated using the formula

$$D = \frac{A_{\parallel} - A_{\perp}}{A_{\parallel} + A_{\perp}} \tag{1}$$

where $A_{\parallel}$ and $A_{\perp}$ are the absorbance values at the maximum for light polarized parallel and perpendicular to the plane of incidence, respectively ($A_{\parallel} > A_{\perp}$).

The linear dichroism can also be derived from the angle of incidence (see Appendix A for details):

$$D_{\alpha} = \frac{2 - \tan^2\beta}{\tan^2\beta \dfrac{1 + \cos^2\alpha}{\sin^2\alpha} + 2} \tag{2}$$

where α is the angle of incidence and β the angle between the transition dipole moment vector ($\vec{\mu}$) and the normal to the plane of the monolayer. Here, we assume that the molecules are distributed uniformly on the surface of the slide with their transition dipole moment vectors forming a constant angle β around the normal.

As can be seen from Eqn. 2, at normal incidence (i.e., $\alpha = 0°$), D_{α} equals zero. Thus there will be no linear dichroism as long as the vectors representing the transition dipole moments of the molecules are uniformly distributed over the surface of the slide and make a constant average angle β with the normal. But, if this uniformity condition is not met, as occasionally was the case for lutein-phosphatidylcholine monolayers, a finite linear dichroism at normal incidence may be recorded. We therefore needed to apply some modifications (shown in Appendix A) to the formulation of the linear dichroism with respect to the angle of incidence, α.

Results

The zeaxanthin and lutein used were tested for purity by thin-layer chromatography (TLC) and were revealed as single spots on an activated silica gel G./dichloromethane/ethylacetate (4:1, v/v) system [34]. An additional trace was sometimes observed probably due to oxidation during TLC. Absorption spectra in ethanol are shown in Fig. 1A (curve 1) for zeaxanthin and Fig. 1B (curve 1) for lutein.

Fig. 2, A and B show the surface pressure-area isotherms (Π-A curves) of zeaxanthin and lutein, respectively (solid lines). The limiting area is 47 $Å^2$/molecule for zeaxanthin and 52 $Å^2$/molecule for lutein. It may be noted that the Π-A isotherm of lutein undergoes a change of slope at around 30 $mN \cdot m^{-1}$, which is absent for zeaxanthin.

For mixed monolayers of lutein and phosphatidylcholine, we have recorded two series of

curves by compressing the film at a rate of 3 $Å^2$/molecule min for one series and 8 $Å^2$/molecule min for the other. Each of these series consisted of eleven *Π-A* curves (the means of three isotherms measured under the same conditions) corresponding to the different molar fractions of lutein (χ_{Lut}) used. Fig. 2B also illustrates the *Π-A* isotherms of mixed monolayers, for a rate of compression of 8 $Å^2$/mol per min. Results for 3 $Å^2$/mol per min (not shown) are of the same pattern. For the sake of clarity, some of the *Π-A* curves have been omitted. The mean molecular area as a function of the molar fraction of lutein is plotted in Fig. 3 for three different surface pressures. The experimental *Π-A* isotherms, within experimental errors, do not follow the additivity rule at any investigated molar fraction. Indeed, at low surface pressures and a low content of lutein, we observed a positive deviation from the additivity rule. As the surface pressure increases (above

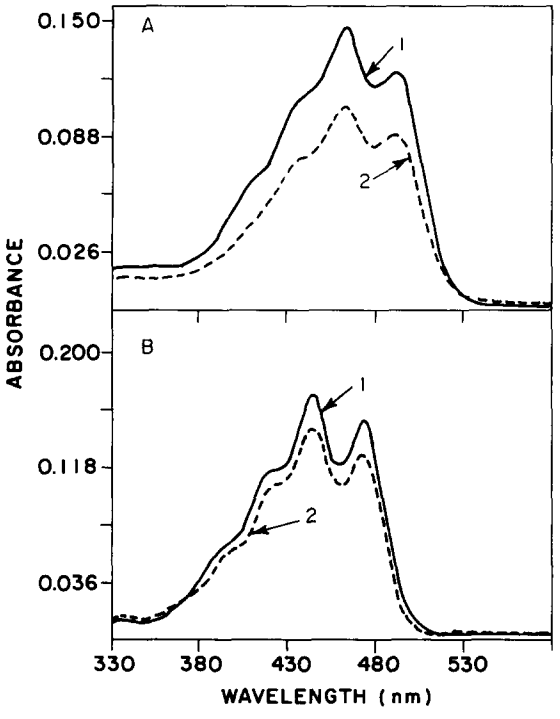

Fig. 1. (A) Absorption spectra of zeaxanthin in ethanol solution (curve 1) and of the zeaxanthin monolayer dissolved in ethanol at the end of spectroscopic measurements (curve 2). (B) Absorption spectra of lutein in ethanol solution (curve 1) and of the lutein monolayer dissolved in ethanol at the end of spectroscopic measurements (curve 2).

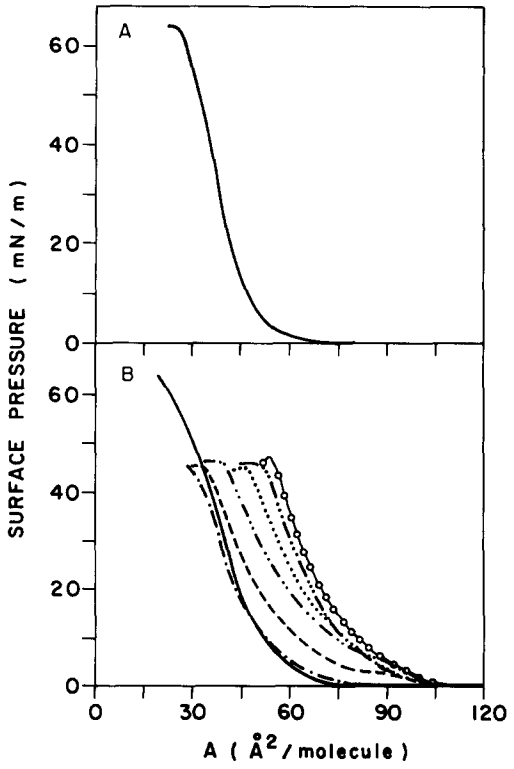

Fig. 2. (A) Pressure-area isotherm of zeaxanthin at air/water interface. Speed of compression: 8 $Å^2$/mol per min. (B) Pressure-area isotherms of pure lutein (———), and of a mixture of lutein and L-α-phosphatidylcholine-β-oleoyl-γ-stearoyl at different molar fraction of lutein: 0.90 (·–·–·), 0.70 (— — —), 0.50 (–··–··), 0.30 (·····) and 0.10 (–···–), and of pure phosphatidylcholine (○———○). Speed of compression: 8 $Å^2$/mol per min.

35 $mN \cdot m^{-1}$), the positive deviation becomes less pronounced or disappears. Instead, at a higher content of lutein, we observed a negative deviation which becomes more pronounced as the surface pressure increases. Except for $\chi_{Lut} = 0.90$, the collapse pressure of mixed monolayers remains the same as for pure phosphatidylcholine (Fig. 2B). Some of the curves of mixed monolayers present regions of very small slope which resemble the plateau observed in *Π-A* isotherms of astaxanthin and canthaxanthin (unpublished data).

The absorption spectra in unpolarized and polarized light of pure zeaxanthin monolayers, deposited at 25 $mN \cdot m^{-1}$, are shown in Fig. 4. Fig. 4A illustrates the results for normal incidence (i.e., $\alpha = 0°$) and reveals no significant differences

between the parallel ($A_{\parallel}$) and perpendicular ($A_{\perp}$) absorption spectra. This absence of linear dichroism indicates a homogeneous distribution of the transition dipole moment vectors of the molecules in the monolayers.

Fig. 4, B and C show the absorption spectra of zeaxanthin monolayers at angles of incidence, α, of 45° and 65°, respectively. In these two cases, absorption of the parallel polarized light exceeds that of perpendicularly polarized light. In each case, the absorption of the unpolarized beam lies, as expected, between those of parallel and perpendicularly polarized beams. Using Eqn. 1 to calculate the linear dichroism, values of 0.20 for $\alpha = 45°$ and 0.41 for $\alpha = 65°$ were obtained. Introduced into Eqn. 2, these values yield corresponding angles, β, of 45.0° for $\alpha = 45°$ and 40.8° for $\alpha = 65°$. Consequently, the angle formed by the transition dipole moment vector with the plane of the monolayer would be 45° for $\alpha = 45°$ and 49.2° for $\alpha = 65°$. Thus β is essentially independent of the angle of incidence.

In Fig 5, the absorption spectra of pure lutein monolayers, deposited at 25 $mN \cdot m^{-1}$, in unpolarized and polarized light are presented. Contrary to those for zeaxanthin, the absorption spectra of lutein monolayers occasionally reveal a small linear dichroism at normal incidence (Fig. 5A) in addition to that observed for $\alpha = 45°$ (Fig. 5B) and $\alpha = 65°$ (Fig. 5C). In these cases, the following formula derived from Eqns. 20 and 21 (Appendix A), was used:

$$D_{\alpha} = \frac{2 + D_N \tan\beta\left(\frac{1+\cos^2\alpha}{\sin^2\alpha}\right) - \tan^2\beta}{2 + \tan^2\beta\left(\frac{1+\cos^2\alpha}{\sin^2\alpha}\right) - D_N \tan^2\beta} \qquad (3)$$

in which D_{α} is the linear dichroism calculated for a finite angle of incidence and D_N is the linear dichroism measured for normal incidence ($\alpha = 0°$). The generalized formula (Eqn. 3) gives values of β which do not differ essentially from those

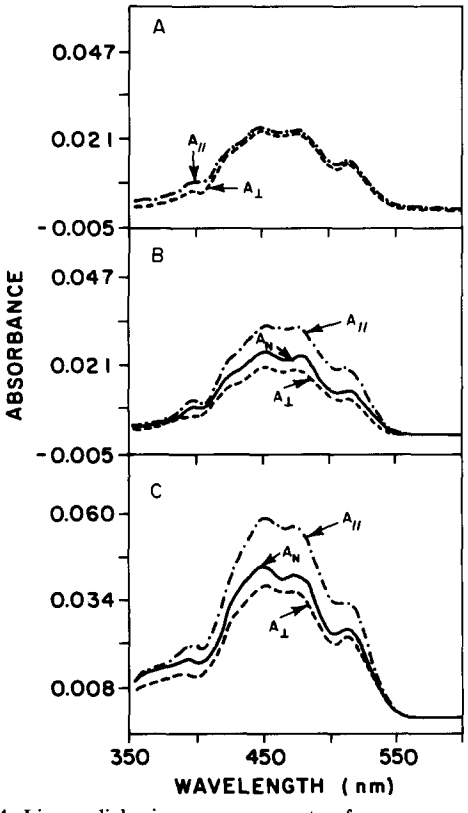

Fig. 4. Linear dichroism measurements of a pure zeaxanthin monolayer at normal incidence (A), at an angle of incidence of 45° (B) and 65° (C). $A_{\perp}$, $A_{\parallel}$ and A_N represent the absorption of perpendicularly, parallel and unpolarized light, respectively.

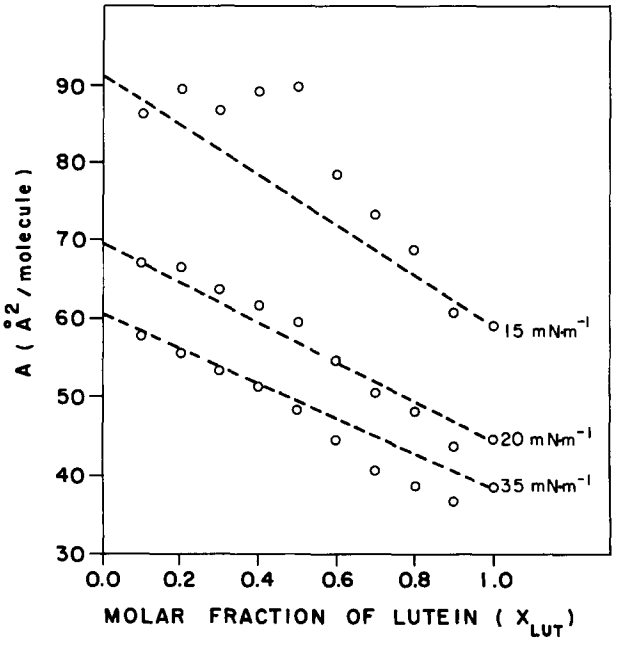

Fig. 3. Molecular area vs. molar fraction of lutein at different surface pressures showing the deviation from the additivity rule.

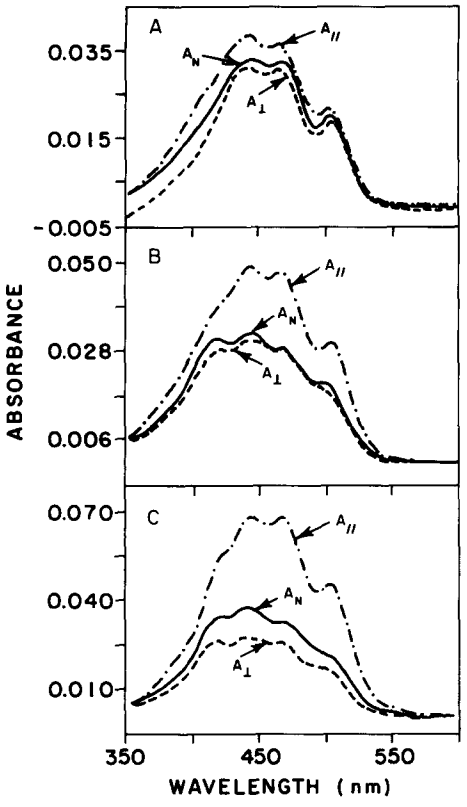

Fig. 5. Linear dichroism measurements of a pure lutein monolayer at normal incidence (A), at an angle of incidence of 45° (B) and 65° (C). The symbols $A_\perp$, $A_{||}$ and A_N have the same meaning as in Fig. 4.

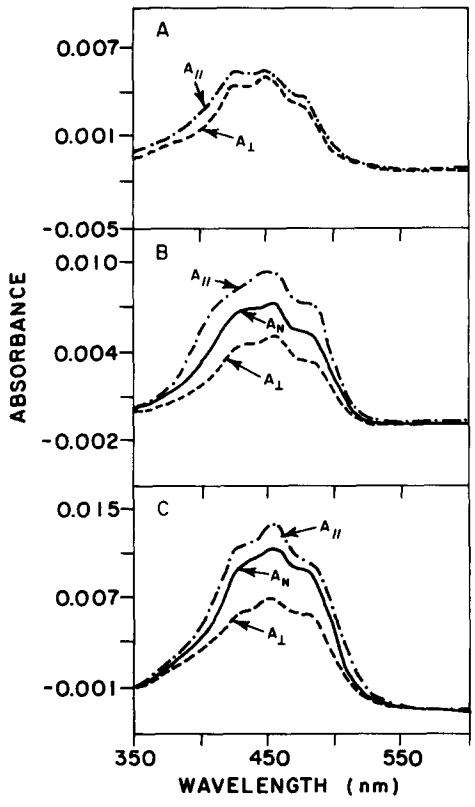

Fig. 6. Linear dichroism measurements of two monolayers of lutein mixed with L-α-phosphatidylcholine-β-oleoyl-γ-stearoyl (1:1, molar ratio) at an angle of incidence of 0° (A), 45° (B) and 65° (C). $A_\perp$, $A_{||}$ and A_N have the same meaning as in Fig. 4.

predicted by the simplified formula (Eqn. 2) mostly used for the calculations. The calculated angle, β, between the transition dipole moment vector and the normal is 44.1° for $\alpha = 45°$ ($D_{45°} = 0.22$) and 38.8° for $\alpha = 65°$ ($D_{65°} = 0.46$). The angle formed by the transition dipole moment vector with the

TABLE I

Sample	Π deposition ($mN \cdot m^{-1}$)	D_N	$D_{45°}$	$D_{65°}$	$\beta_{45°}$	$\beta_{65°}$	$\bar{\beta}$	Relative deviation (%)
Zeaxanthin	25	0.00	0.20		45.0			
	25	0.00		0.41		40.8	42.9	9.8
Lutein	25	0.00	0.22		44.1			
	25	0.00		0.46		38.8	41.4	12.8
Lutein/PC (1:1)	5	0.00	0.26		42.4			
	5	0.00		0.43		40.0	41.2	5.8
	25	0.00	0.25		42.8			
	25	0.00		0.39		41.5	42.1	3.1
	40	0.02	0.24		43.8			
	40	0.02		0.44		40.0	41.9	9.0

plane of the monolayer is therefore 45.9° for $\alpha = 45°$ and 51.2° for $\alpha = 65°$. These are the mean values of at least three results obtained with different preparations.

Fig. 1 shows the absorption spectra of the zeaxanthin (Fig. 1A, curve 2) and lutein (Fig. 1B, curve 2) monolayers, redissolved in ethanol at the end of the experiments. No change in the spectra compared with those of the corresponding fresh solutions is indicated, attesting to no damage to the compounds during the experiments.

Concerning mixed monolayers of lutein and L-α-phosphatidylcholine-β-oleoyl-γ-stearoyl (1 : 1, molar ratio), the linear dichroism is essentially the same as that of the pure lutein monolayer. Table I shows data obtained for different angles of incidence and surface pressures of deposition, together with results obtained for pure compounds. The angle β varies from 40° to 43.8° for the mixed monolayers. The absorption spectra of the mixed monolayers deposited at 25 $mN \cdot m^{-1}$ are presented in Fig. 6.

As could be seen in Fig. 2B, a plateau was present in the *Π-A* isotherms of mixed monolayers of lutein and lecithin at low surface pressures. It was therefore of interest to investigate the state of the mixed monolayer below and above the plateau region. Accordingly, the mixed monolayer was deposited on the quartz disks at a surface pressure of 5 $mN \cdot m^{-1}$ (below the plateau) and at 25 $mN \cdot m^{-1}$ (above the plateau). The absorption spectra of these monolayers are shown in Fig. 7.

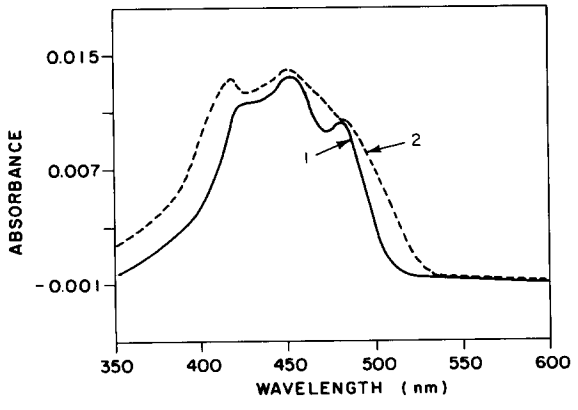

Fig. 7. Absorption spectrum of two monolayers of a mixture of lutein and L-α-phosphatidylcholine-β-oleoyl-γ-stearoyl (1 : 1, molar ratio) deposited at 5 $mN \cdot m^{-1}$ (curve 1) compared with that deposited at 25 $mN \cdot m^{-1}$ (curve 2).

Discussion

The almost unchanged collapse pressure (Fig. 2B) for $0.00 \leq \chi_{Lut} \leq 0.80$ provides evidence that, at least at high surface pressure, a significant part of the mixed film has the same properties as the pure phosphatidylcholine monolayer. This would suggest that phosphatidylcholine and lutein are not fully soluble in one another. On the other hand, experimental values of the mean molecular areas at 35 $mN \cdot m^{-1}$ for $\chi_{Lut} = 0.10$, 0.20 and 0.30 are close to the values predicted by the additivity rule. It seems reasonable to conclude that for the above values of χ_{Lut} at surface pressures higher than 35 $mN \cdot m^{-1}$, phosphatidylcholine and lutein form two separated phases. From microscopic observations (unpublished data), lutein and zeaxanthin, when spread without compression on the water surface at a molecular area of 50 $Å^2$/molecule, do not seem truly monomolecular. Most probably, under these conditions at least, the lutein film has a porous polycrystalline structure. On the Langmuir trough, above 35 $mN \cdot m^{-1}$, parallel and orange-coloured thread formations were observed with the naked eye. The negative deviation from the additivity rule, for higher lutein molar fractions, suggests the presence of pinholes in the lutein polycrystalline network that are filled with phosphatidylcholine monolayers.

The positive deviations from additivity at low surface pressure are due to the plateau observed in experimental *Π-A* isotherms of mixed monolayers. Such a plateau, observed previously in pure films of canthaxanthin and astaxanthin, was considered to be due to crystallization (unpublished data). Molecules of astaxanthin and canthaxanthin may interact with the water surface at both ends. The work which has to be performed in breaking the hydrogen bond between water and one of the ends of the carotenoid molecule, constitutes an activation barrier for crystallization. As a result, the crystallization is a relatively slow process at zero surface pressure. Compression and the rise of surface pressure accelerate crystallization. The process takes place at a surface pressure measurably different from zero and is reflected by the plateau in the *Π-A* isotherm.

We have never observed a plateau in the *Π-A* isotherms of one-component films of echinenone,

hydroxyechinenone and β-cryptoxanthin. Molecules of these three carotenoids have a hydrophilic group at one end only. Consequently, the other end is not attached to water and there is no activation barrier for crystallization. In virtue of this, crystallization is quite a rapid process at zero surface pressure. After crystallization, the surface pressure becomes measurable, and no plateau can be observed for these carotenoids.

The absence of a plateau in the *Π-A* isotherms of lutein and zeaxanthin films may be explained by the geometry of these molecules, which prohibits their interaction with water at both ends simultaneously. Consequently, surface films of these compounds behave more like those of one-head carotenoids than those of canthaxanthin and astaxanthin. If the crystallization hypothesis is correct, then the presence of a plateau in the *Π-A* isotherms of mixed monolayers of lutein and phosphatidylcholine can be accounted for by the following two mechanisms. First, the presence of phosphatidylcholine molecules, especially at small lutein molar fractions, makes collisions between two or more molecules of lutein less probable. If this is so, then the surface pressure corresponding to the plateau should be higher at smaller molar fraction of lutein. Such a tendency is clearly indicated in Fig. 2B. Second, lutein molecules can form hydrogen bonds with β and/or α-ester bond oxygens of the phosphatidylcholine molecules. Such bonds would indirectly attach the free end of a lutein molecule to water, and would create an activation barrier for crystallization.

The spectroscopic results that we have obtained show that each of the carotenoid monolayer studied possesses a significant linear dichroism. This is true both for the pure compounds and for the lutein-phosphatidylcholine mixtures, and was measurable at angles of incidence of 45° and 65°. At normal incidence, there was no linear dichroism for zeaxanthin, and only a little dichroism for lutein and lutein-phosphatidylcholine mixture in some experiments. The latter could stem from an imperfectly homogeneous distribution of the molecules at the air/solid interface. In all cases, the angle between the transition dipole moment vector and the plane of the support is in the range 45° to 51°. Difference between the values obtained at different angles of incidence is quite insignificant considering the low absorbance levels measured (0.01–0.08) and their accompanying mean deviation of around 8%.

The preceding discussion on crystallization implies that the film is in different states on each side of the plateau. However, there is no significant difference between the dichroism results obtained at low surface pressure (5 $mN \cdot m^{-1}$) and those obtained at high surface pressure (25 and 40 $mN \cdot m^{-1}$), as indicated in Table I. There is no significant difference in the absorption spectra (Fig. 7). The absorption spectra are rather indicative of monomers [35], though for pure lutein and zeaxanthin monolayers, shifts of the main absorption band to near 410 nm, characteristic of a crystalline [15,35] or aggregate state [36] were occasionally observed. It is therefore reasonable to conclude that partial crystallization occurs, maybe in microdomains in the monolayer phase, and to link this process with the plateau in the *Π-A* isotherms and with the observed deviations from additivity.

How important are the dichroic properties and orientation of the carotenoids in vivo? For carotenoids, the absorption dipole moments usually lie along the long molecular axis [37–41]. Thus the carotenoid molecules involved in the present study appear to lie at a mean angle of 48° to the surface of the solid support. These findings, which are consistent with results reported elsewhere on carotenoid monolayers [25,26] in the sense that the carotenoid molecules form an acute angle to the plane of the membrane, differ, however, quantitatively from the published data. Indeed, the angle we obtained is quite a lot higher than that reported in several cited references [25,26]. Reich et al. [25] have measured an angle of 16° for total carotenoids in chloroplast, which is a different system, using electrochromic methods. Although it is not surprising that our results differ greatly from those of Reich et al. [25] because of difference between the systems studied, one may question the accuracy of the electrochromic methods they used. We believe that the linear dichroism, being a direct measuring method, applied to a well defined system (i.e., Langmuir-Blodgett films) is more appropriate for this study. Applying resonance Raman spectroscopy to a different carotenoid system, i.e., β-carotene and phosphati-

dylcholine, Van de Ven et al. [27] found that in soybean phosphatidylcholine bilayers, β-carotene is oriented perpendicular to the bilayer plane while it lies parallel to the plane in dioleoylphosphatidylcholine bilayer. In another study involving the linear dichroism of chloroplast membranes, Breton and his co-workers [16,17,18] concluded that carotenoids (mainly β-carotene) in spinach chloroplasts lie close to the lamellar plane. These observations could be expected since β-carotene has no polar head group.

Our results are in accordance with those of Snodderly et al. [42], who applied microspectrometry to retinal tissue. It was shown that the macular tissue, which contains lutein and zeaxanthin [11], was dichroic. The greatest absorption occurred when the plane of polarization of the incident light was perpendicular to the axes of the Henlé fibers, thereby accounting for the formation of Haidinger's polarization brushes. In another paper [15], it has been shown that the brushes can be explained by a model which supposes a fraction of the carotenoid molecules to be aligned perpendicular to the cylindrically shaped fiber membranes. The remainder was assumed to have random orientations. In the light of the present results, an alternative interpretation would be that all the molecules are disposed about some average angle to the membrane surface. We have calculated that, for a fiber as a whole to absorb light more strongly which is polarized perpendicular to its axis, rather than parallel, this angle would have to exceed approximately 35°. Our measured angles are all equal to or greater than 45° and, as such, are completely consistent with these calculations and with the measurements of Snodderly et al.'s [42]. In addition, it may be noted that the lutein monolayers reproduce the absorption band in retinal tissue, which is centered at 460 nm [43].

Conclusion

Dichroic and orientational measurements of lutein, zeaxanthin and mixtures of lutein and phosphatidylcholine have been carried out in Langmuir-Blodgett films. The results obtained, which are in excellent agreement with observations reported on the native macular tissue, indicate that the carotenoid molecules are oriented at a mean angle of 48° to the surface of the support of the film. It is inferred that carotenoid molecules in the macula form an angle of the same magnitude to the surface of the membrane of Henlé fibers. One important point, concerning the relationship between these carotenoid molecules and the membrane constituents of the Henlé fibers remains, however, to be clarified.

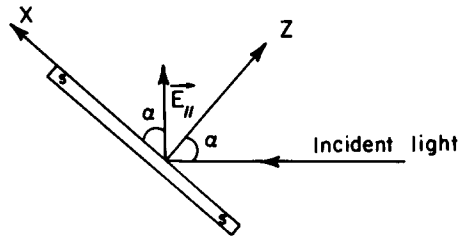

Fig. 8. Geometry of the linear dichroism measurements. S is the slide. Axis Z is normal to the plane of the slide (monolayer). Axes X and Y are in the plane of the slide: X is a horizontal, and Y a vertical axis. α is the angle of incidence. $\vec{E}_{\parallel}$ is the electric vector of the parallel polarized light.

Appendix A

The measurements of linear dichroism of deposited monolayers were performed in the geometry presented in Fig. 8. Derivation of the formulas used in the text is based on the assumption that all transition dipole moments (long axes of the carotenoid molecules) form the same angle β with the normal to the plane of the slide. The distribution of orientations of transition dipoles in the XY plane is expected to be almost homogeneous. However, vertical movement of the quartz slide during deposition can disturb this homogeneity. Therefore we suppose that, in the general case, the orientation of molecules in the XY plane is described by a distribution $N(\psi)$, which satisfies Eqns. 4 and 5:

$$\int_0^{\pi} N(\psi)\, \mathrm{d}(\psi) = 1 \tag{4}$$

$$N(\psi) = N(\pi - \psi) \tag{5}$$

where ψ is the angle between the X axis and the projection of the transition dipole on the XY plane. Eqn. 4 is an obvious normalization condi-

tion. Eqn. 5 implies that the distribution $N(\psi)$ is symmetrical with respect to the vertical Y axis. Such properties of the distribution are highly probable, because the orientation of the slide was the same during deposition and during optical measurements.

The probability of absorption of a quantum by the carotenoid molecule is proportional to $\cos^2\gamma$, where γ is the angle between the transition dipole moment of a molecule and the electric vector of the incident light wave. First, we calculate cos γ as a scalar product of two unit vectors. One of these vectors is parallel to the transition dipole, the other is parallel to the electric field intensity vector of the light wave. Next, we calculate the average value of $\cos^2\gamma$ and finally derive an expression for linear dichroism according to Eqn. 2:

$$D = \frac{\langle\cos^2\gamma\rangle_{\parallel} - \langle\cos^2\gamma\rangle_{\perp}}{\langle\cos^2\gamma\rangle_{\parallel} + \langle\cos^2\gamma\rangle_{\perp}} \tag{6}$$

where indices $_{\parallel}$ and $_{\perp}$ correspond to the parallel and perpendicular planes of polarization of the light wave. Provided that the proportionality coefficient between $\cos^2\gamma$ and absorption is the same for both polarizations, Eqn. 6 is identical with the definition of linear dichroism used in the text. Under such assumptions we can write:

$$\vec{\mu} = (\sin\beta\cos\psi, \sin\beta\sin\psi, \cos\beta) \tag{7}$$

$$\vec{E}_{\perp} = (0, 1, 0) \tag{8}$$

$$\vec{E}_{\parallel} = (\cos\alpha, 0, \sin\alpha) \tag{9}$$

where $\vec{\mu}$, $\vec{E}_{\parallel}$, $\vec{E}_{\perp}$, are unit vectors parallel respectively to the transition dipole moment and to the electric field of the light wave under the two polarization conditions. So, for perpendicular polarization of the electric vector, we have

$$\cos\gamma_{\perp} = \vec{E}_{\perp}\cdot\vec{\mu} = \sin\beta\sin\psi \tag{10}$$

and

$$\langle\cos^2\gamma\rangle_{\perp} = \sin^2\beta\langle\sin^2\psi\rangle \tag{11}$$

where

$$\langle\sin^2\psi\rangle = \int_0^{\pi} N(\psi)\sin^2\psi\,\mathrm{d}\psi \tag{12}$$

From Eqns. 4, 11 and 12 it follows that,

$$\langle\cos^2\gamma\rangle_{\perp} = \sin^2\beta\left(\tfrac{1}{2} - \tfrac{1}{2}I\right) \tag{13}$$

where

$$I = \int_0^{\pi} N(\psi)\cos^2\psi\,\mathrm{d}\psi \tag{14}$$

For the parallel polarization we have:

$$\cos\gamma_{\parallel} = \vec{E}_{\parallel}\cdot\vec{\mu} = \sin\beta\cos\psi\cos\alpha + \cos\beta\sin\alpha \tag{15}$$

and

$$\langle\cos^2\gamma\rangle_{\parallel} = \sin^2\beta\cos^2\alpha\langle\cos^2\psi\rangle + 2\sin\beta\cos\beta\sin\alpha\cos\alpha\langle\cos\psi\rangle + \cos^2\beta\sin^2\alpha \tag{16}$$

where

$$\langle\cos^2\psi\rangle = \int_0^{\pi} N(\psi)\cos^2\psi\,\mathrm{d}\psi = \tfrac{1}{2} + \tfrac{1}{2}I \tag{17}$$

and

$$\langle\cos\psi\rangle = \int_0^{\pi} N(\psi)\cos\psi\,\mathrm{d}\psi = 0 \tag{18}$$

because of Eqn. 5.

So

$$\langle\cos^2\gamma\rangle_{\parallel} = \sin^2\beta\cos^2\alpha\left(\tfrac{1}{2} + \tfrac{1}{2}I\right) + \cos^2\beta\sin^2\alpha \tag{19}$$

Inserting Eqns. 13 and 19 into Eqn. 6 we obtain:

$$D = \frac{2\cos^2\beta\sin^2\alpha + \sin^2\beta(1+\cos^2\alpha)I - \sin^2\beta\sin^2\alpha}{\sin^2\beta(1+\cos^2\alpha) + 2\cos^2\beta\sin^2\alpha - I\sin^2\beta\sin^2\alpha} \tag{20}$$

For light at normal incidence $\alpha = 0°$ and it follows from Eqn. 20 that:

$$D_N = I \tag{21}$$

It is not necessary to know the distribution, $N(\psi)$, in order to calculate the linear dichroism at finite angles of incidence. In order to evaluate integral, I, in Eqn. 20, we can measure the linear dichroism at normal incidence and make use of Eqn. 21. In the event that the linear dichroism at

normal incidence is zero (then $I = 0$), we can divide the numerator and denominator of Eqn. 20 by $\cos^2\beta \sin^2\alpha$ to obtain a simpler formula:

$$D_\alpha = \frac{2 - \tan^2\beta}{\tan^2\beta\left(\frac{1+\cos^2\alpha}{\sin^2\alpha}\right) + 2} \quad (22)$$

In any case insertion of experimentally determined values of D_N, D_α and α into Eqns. 22 or 20 and 21 leads to the linear equation for $\tan^2\beta$.

Acknowledgments

The authors would like to express their gratitude to Miss Louise Leblanc for her assistance in performing part of this study. This work was supported by the Natural Sciences and Engineering Research Council of Canada and the Fonds pour la Formation de Chercheurs et l'Aide à la Recherche.

References

1 Ditchburn, R.W. (1973) in Eye-Movement and Visual Perception, Clarendon Press, Oxford.
2 Krinsky, N.I. (1976) in Symp. Soc. Gen. Microbiol. Survival of Vegetative Microbes (Gray, T.G.R. and Postgate, J.R., eds.), pp. 209–239, Cambridge University Press, Cambridge.
3 Krinsky, N.I. (1979) Pure Appl. Chem. 51, 649–660.
4 Giese, A.C. (1971) Photophysiology 6, 77–129.
5 Kirschfeld, K. (1982) Proc. R. Soc. Lond. B 216, 71–85.
6 Krinsky, N.I. (1968) Photophysiology 3, 123–195.
7 Krinsky, N.I. (1971) in Carotenoids (Isler, O., Gutmann, H. and Solms, U., eds.), pp. 669–710, Birkhäuser Verlag, Basel.
8 Rodieck, R.W. (1973) The Vertebrate Retina, W.H., Freeman, San Francisco.
9 Nussbaum, J.J., Pruett, R.C. and Delori, F.C. (1981) Retina 1, 296–310.
10 Wolbarsht, M.L. (1976) Fed. Proc. FASEB 35, 4450.
11 Bone, R.A., Landrum, J.T. and Tarsis, S.L. (1985) Vision Res. 25, 1531–1535.
12 Snodderly, D.M., Auran, J. and Delori, F.C. (1979) Invest. Ophtalmol. Vis. Sci. 18 (Suppl.), 80.
13 De Vries, H.L., Spoor, A. and Jielof, R. (1953) Physica Utrecht 19, 419–432.
14 Delori, F.C., Webb, R.H. and Parker, J.S. (1979) Invest. Ophthalmol. Vis. Sci. 18 (Suppl.), 53.
15 Bone, R.A. and Landrum, J.T. (1984) Vision Res. 24, 103–108.
16 Breton, J. and Roux, E. (1971) Biochem. Biophys. Res. Commun. 45, 557–563.
17 Breton, J., Michel-Villaz, M. and Paillotin, G. (1973) Biochim. Biophys. Acta 314, 42–56.
18 Becker, J.F., Breton, J., Geacintov, N.E. and Trentacosti, F. (1976) Biochim. Biophys. Acta 440, 531–544.
19 Geacintov, N.E., Van Nostrand, F. and Becker, J.F. (1974) Biochim. Biophys. Acta 347, 443–463.
20 Goedheer, J.C. (1955) Biochim. Biophys. Acta 16, 471–476.
21 Kolev, V.D. and Kafalieva, D.N. (1985) C.R. Acad. Bulg. Sci. 38, 755–758.
22 Rohmer, M., Bouvier, P. and Ourisson, G. (1979) Proc. Natl. Acad. Sci. USA 76, 847–851.
23 Yamamoto, H.T. and Bangham, A.D. (1978) Biochim. Biophys. Acta 507, 119–127.
24 Ohnishi, T., Hatakeyama, M., Yamamoto, N. and Tsubomura, H. (1978) Bull. Chem. Soc. Japan 51, 1714–1716.
25 Reich, R., Scheerer, R., Sewe, K.-U. and Witt, H.T. (1976) Biochim. Biophys. Acta 449, 285–294.
26 Sewe, K.-U. and Reich, R. (1977) Z. Naturforsch. 32c, 161–171.
27 Van de Ven, M., Kattenberg, M., van Ginkel, G. and Levine, Y.K. (1984) Biophys. J. 45, 1203–1210.
28 Britton, G. and Goodwin, T.W. (1971) in Methods in Enzymology, Vol. 18 (McCormick, D.B. and Wright, L.D., eds.), pp. 654–701, Academic Press, New York.
29 Strain, H.H. (1938) Leaf Xanthophylls, Carnegie Institution of Washington, DC.
30 Braumann, E. and Grimme, H.L. (1981) Biochim. Biophys. Acta 637, 8–17.
31 Heller, F.R. and Milne, G.W.A. (1978) ETA/NIH Mass. Spectral Data Base, Vol. 4, National Bureau of Standards, Washington.
32 Hager, A. and Meyer-Bertenrath, T. (1966) Planta 69, 198–217.
33 Munger, G., Lorrain, L., Gagné, G. and Leblanc, R.M. (1987) Rev. Sci. Instrum. 58, 285–288.
34 Bolliger, H.R. and König, A. (1969) in Thin-Layer Chromatography (Stahl, E., ed.), pp. 259–311, Springer-Verlag, New York and Berlin.
35 Mendelsohn, R. and Van Holten, R.W. (1979) Biophys. J. 27, 221–236.
36 Takagi, S. and Takeda, K. (1983) Agric. Biol. Chem. 47, 1435–1440.
37 Hoskins, L.C. (1981) J. Chem. Phys. 74, 882–885.
38 Warshel, A. and Dauber, P. (1977) J. Chem. Phys. 66, 5477–5488.
39 Ho, Z.Z., Hanson, R.C. and Lin, S.H. (1982) J. Chem. Phys. 77, 3414–3423.
40 Siebrand, W. and Zgierski, M.Z. (1979) J. Chem. Phys. 71, 3561–3569.
41 Lukashin, A.V. and Frank-Kamenetskii, M.D. (1978) Chem. Phys. 35, 469–476.
42 Snodderly, D.M., Auran, J.D. and Delori, F.C. (1984) Invest. Ophthalmol. Vis. Sci. 25, 674–685.
43 Snodderly, D.M., Brown, P.K., Delori, F.C. and Auran, J.D. (1984) Invest. Ophthalmol. Vis. Sci. 25, 660–673.